Pis'ma v ZhETF, vol.62, iss.6, pp.483 - 490

TEMPERATURE DEPENDENCE OF RESISTIVITY AND STRUCTURE OF CARBON NANITUBE FILMS CONTAINING VARIOUS KINDS OF TUBULES

O.E.Omel'yanovskii, V.I.Tsebro[1)], *O.I.Lebedev*[+], *A.N.Kiselev*[+], *V.I.Bondarenko*[+], *N.A.Kiselev*[+], *Z.Ja.Kosakovskaja*[*], *L.A.Chernozatonskii*[□]

Lebedev Physical Institute RAS
117924 Moscow, Russia

[+] *Institute of Crystallography RAS*
117334 Moscow, Russia

[*] *Institute of Radio Engineering and Electronics RAS*
103907 Moscow, Russia

[□] *Institute of Chemical Physics RAS*
117977 Moscow, Russia

Submitted 9 August 1995

The temperature dependence of the resistivity over the range of 4.2 to 300K has been measured on the carbon films containing multilayer nanotubes (MLT) or single layer nanotubes (SLT) oriented perpendicularly to the substrate. The structure of these films has been examined by high resolution electron microscopy. At low temperatures, the planar resistivity of all the films is well-fitted by the expression $\ln\rho \propto [T_0/T]^{1/n}$ with $n = 4$ and $T_0 \sim 10^6$ K for the MLT films, but with $n = 2$ and $T_0 \sim 20$ K for the films containing the bundles of SLT of 0.71 nm in diameter. The data obtained are considered in terms of the variable-range hopping conductivity. The estimations made show a fairly high density of states at the Fermi level ($\sim 10^{21}$ $eV^{-1} \cdot cm^{-3}$) for the films containing SLT's.

Since the discovery of carbon nanotubes (buckytubes) [1] their electronic properties have been of great interest. Most studies are band structure calculations for single nanotubes (see, for example, review [2]). It follows from these studies that the type of electronic structure is subject to variation from metallic to semiconducting depending on the tubule diameter and the degree of helical arrangement. There have been experimental researches devoted to longitudinal conductivity of nanotube bundles [3, 4]. In Ref. [3], the conductivity of a big multiple bundle of several tens of microns in diameter has been investigated, while the resistance of a single carbon nanotube bundle $\sim$ 50 nm in diameter has been successfully measured using "state-of-the-art" technique by R. Langer and co-workers [4]. In general terms, both works showed a semimetallic conductivity of buckytubes with weak localization behavior at low temperatures.

A variety of techniques has been used to demonstrate the possibility of buckytube films producing by electron beam evaporation of graphite [5–9]. Among them scanning tunneling microscopy (STM) was most often used [5, 6, 8, 9]. In particular, STM revealed that the surface relief of the films obtained at medium densities of carbon flow is formed by dome shaped and/or conical tips. In the films obtained under slightly different conditions, STM showed a surface relief consisting of rods 1 nm in diameter [6]. High-resolution electron microscope (HREM) imaging was used to examine the films deposited on different substrates at medium carbon

[1)]e-mail: tsebro@sci.lpi.ac.ru

flow [7]. Most of them did consist of multilayered nanotubes (MLT). Scanning electron microscope (SEM) imaging of broken films revealed a fiber structure oriented toward carbon flow [6, 8]. Such a structure is most probably formed by the aggregates of MLT's or by the bundles of single layer nanotubes (SLT). The bundles of SLT's were first observed by N. Kiselev and others [10] in those films where STM revealed 1 nm rods. As was mentioned in Ref. [11], the kind of buckytube structure, besides the carbon flow density, is also affected by the type of substrate and its temperature as well as vacuum condition and arrangement of deposition process.

The purpose of this paper is to provide an experimental study of the structure and the temperature dependence of the resistivity of the same buckytube films prepared under different conditions and, hence, having considerably different structures. Buckytube films were deposited on (111)Si and glass substrates using electron beam deposition technique described elsewhere [5, 6]. During the deposition process, the carbon flow was directed normally to the substrate. Hence the orientation of nanotubes is expected to be normal to the plane of the substrate. For all investigated films the type of substrate and film thickness (t_f) are given in Table. For sample #4 the deposition process was interrupted, so that in the data given below the considerable difference in its properties is seen.

sample	substrate	t_f,nm	D,nm	n_l	ρ(250K/25K/5K)	n	T_0,K	T^*,K
#1	glass	150	0.72	1 [a]	0.014/0.039/0.11	2	16	15
#2	glass	170	0.72	1 [a]	0.0086/0.023/0.074	2	23	25
#3	(111)Si	93	≤ 25	11–34	0.26/180/250000 [c]	4	$1.1 \cdot 10^6$	165
#4	glass	120	0.72	1 [b]	0.0052/0.011/0.019	4	39	48

[a] bundles of STL's; [b] separate SLT's; [c] obtained by extrapolation.

The specimens for HREM were prepared by scrapping the film of the substrate. Detached fragments were ultrasonificated in acetone. The imaging were taken in a Philips EM 430ST instrument operated at 200 kV. Computer simulation based on the multislice method [12] was used for image interpretations.

According to HREM examination of the film deposited on (111)Si (sample #3), the main component of the film is MLT's like those observed by Iijima [1]. The number of layers in these MLT's ranges from 11 to 32. The length of tubules is comparable to the film thickness. In many cases, HREM imaging demonstrates the outer layers of nanotubules being destroyed. In some instances one can observe an external amorphous layer. An example of MLT from this specimen is shown in Fig. 1*a*.

Another type of structure (Fig. 1*b*) was observed in the films deposited onto the glass substrate under those conditions just when STM revealed a rod relief (samples #1 and #2) [5, 6]. This type can be characterized as a buckytube bundle with longitudinal striation having a periodicity of 1.06 nm. The maximal length of the bundles is also comparable with the film thickness. In addition to this major periodicity, HREM imaging revealed a finer structure which has been pronounced as additional longitudinal bands of various contrast. In some images an "oblique" periodicity running at an angle to the bundle axis was observed.

The following assumptions, subsequently tested by computer simulation, have been made: (1) the observed bundles are formed by 100 – 1000 SLT's (also, see Ref. [10]); (2) these nanotubes do not have any intermediate layers and form close, probably, hexagonal packing; (3) adjacent nanotubes are shifted with respect to one another in a certain order, i.e. the bundle can be considered as a quasicrystal.

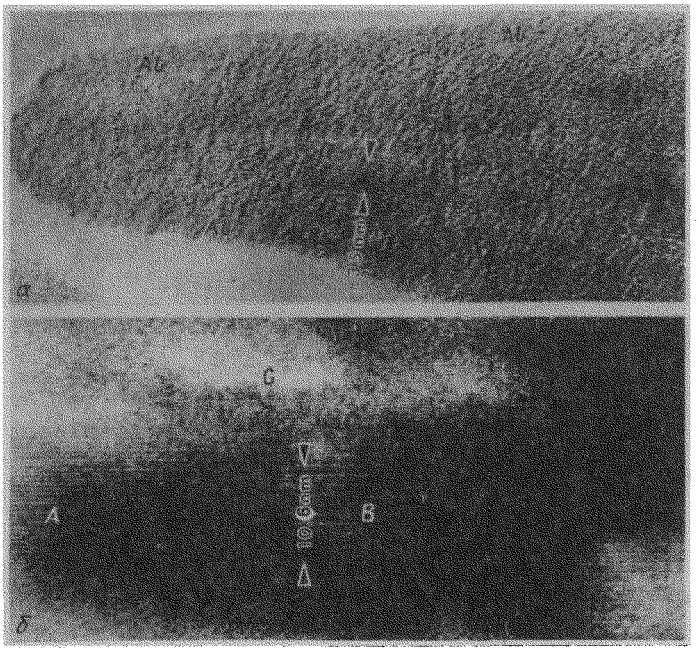

Fig.1. HREM images of carbon nanotubes films: (*a*) a covered by an amorphous layer (AL) MLT from the film on (111)Si substrate ; (*b*) a bundle of SLT's from the film on the glass substrate. Marked by *A*, *B*, and *C* are the regions of different contrast

For image simulation, one of the possible packing of hexagons, so called "zigzag", as well as the chiral angle $\theta = 0$, were used [2, 13]. Such a zigzag tubule, having a tubular diameter of 0.71 nm, is formed of the rings of 9 hexagons each. The choice of parameters for simulation is governed by the observed periodicity (1.06 nm) and the distance between carbon layers or, more properly, the walls of the tubules (0.35 nm).

The image simulation has been fulfilled for two versions of mutual orientation of the closely packed tubes. In the first version, the packing is assumed to be a simple translation of the tubes. In this case, a certain similarity with the experimental images has been obtained, but the oblique periodicity cannot be explained. In the second version, one of the tubes in the unit cell is turned through 20°, and the other one is shifted along the axis. Just then, the oblique periodicity is observed at certain defocus Δf and specimen thickness t. Various kinds of HREM images as well as the selected image simulations are presented in Fig. 2.

The analysis of image simulations allows the decision to be made that the above structure model does not conflict with the experimental data, i.e. the observed structure can be really considered as the bundles of hexagonally packed zigzag nanotubes 0.71 nm in diameter and the chiral vector (9,0).

In the micrographs, the SLT bundles are set out with a pronounced contrast, so that their images must result from the superposition of a few nanotubes. On the other hand, the computer simulation images resembling the experimental ones with oblique periodicity correspond only to small thicknesses (0.8 – 1.3 nm). This contradiction could be explained by assuming that the bundles are tilted to the electron beam through 5 – 15°. In this case, a preliminary image simulation already shows that the oblique periodicity is revealed at greater thicknesses.

The hexagonal packing and cylindrical shape of the nanotubes is not the only version of possible tentative design of the bundles. A rectangular packing of tubules, having hexagonal cross-section, has been also considered. In this case,

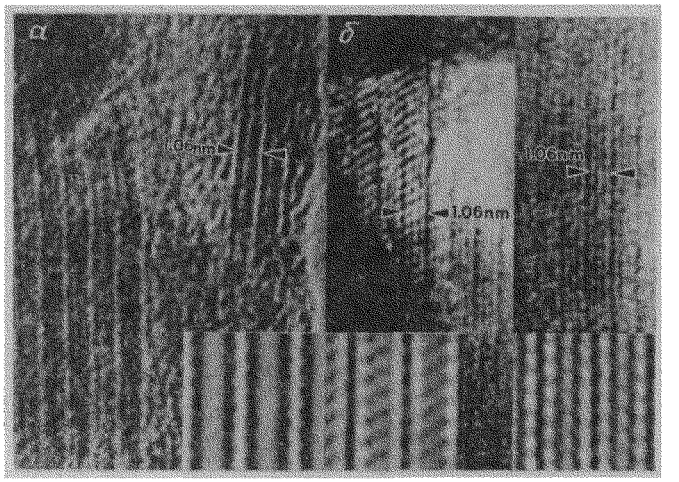

Fig.2. HREM images of the different kinds of SLT bundles. Shown at the bottom are simulated images along [110]: (*a*) $t = 2.4$ nm, $\Delta f = -20$ nm; (*b*) $t = 1.3$ nm, $\Delta f = -10$ nm; (*c*) $t = 0.8$ nm, $\Delta f = -10$ nm (see designations in text)

the contrast of the tube walls in the simulated images is increased as well as the visibility of the inner oblique structure.

The above interpretation of the experimental images as the bundles of SLT's seems to be the best one. Nevertheless the striated structure containing moire fringes could be also obtained within the fibrillar model when the bundle is formed by carbon ribbons, or within the lamellar model when these fringes originate from a bent carbon layer [14]. However, in both cases the expected striation periodicity is much larger that in our experimental micrographs. Besides this, both models seemingly do not explain STM data [5, 6, 8, 9]. It seems that the final judgment about the type of observed structure could be made after the analysis of electron diffraction patterns and plain-view HREM investigations of the films.

It should be noted that the nanotubes comprising the bundles are sensitive to radiation damage. The effect of electron beam on relatively small bundles and separate tubules is more pronounced. Along with SLT's a small amount of fullerite C_{60} crystals was revealed. In sample #4 mentioned above (corrupted deposition process), the bundles of nanotubes were not observed but, instead, a small quantity of SLT's of approximately 0.71 nm in diameter appeared. They were surrounded by a structureless, perhaps amorphous material. As shown below, the temperature dependence of the resistivity of this film is principally different from that of the films containing nanotube bundles.

Measurements of the resistivity ρ (over the temperature range from 4.2 to 300 K) were carried out on the same samples the structure of which was concurrently investigated by HREM. There was used standard dc four-probe method. Electrical contacts with the films which measure $\sim 2 \times 12$ mm, were made by silver epoxy. It is apparent that having the nanotube axes normal to the substrate or slightly tilted to it, the film passed the current across the tube axes.

It turned out that, at temperatures below a certain value (T^*), all the films precisely exhibit the temperature-dependent resistivity $\rho(T)$ of the form

$$\rho(T) = \rho_0 \exp\left[(T_0/T)^{1/n}\right] , \qquad (1)$$

typical of variable-range hopping (VRH) mechanism. However, the various types of films showed up the radically different $\rho(T)$ dependencies in magnitudes of n and T_0 in the Eq. (1).

Thus the films containing multilayered nanotubes are characterized by rather high values of the resistivity at low temperature, the many-decade temperature dependence of which is a characteristic of a strongly localized system. At $T <$ 150 – 200 K, the $\rho(T)$ dependence of these films strictly follows Eq. (1) with n = 4. The value of T_0 exceeds 10^6 K. As an example, the logarithmic resistivity versus $T^{-1/4}$ for sample #3 is shown in Fig. 3 (left scale).

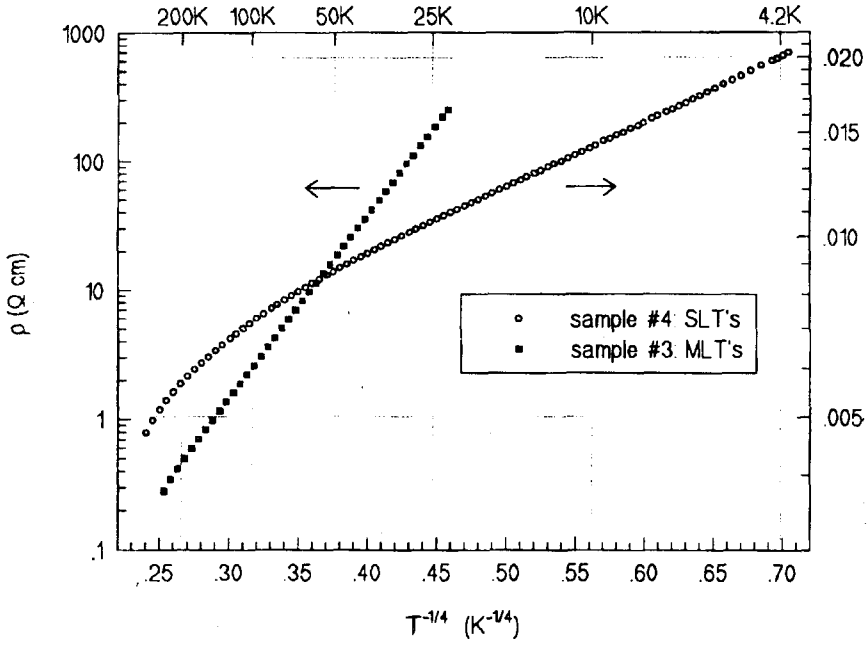

Fig.3. Logarithmic resistivity versus $T^{-1/4}$ for the film with MLT's (left scale) and for the film with separate SLT's (right scale)

On the other hand, the films containing the bundles of SLT's have significantly lower resistivity, and their $\rho(T)$ dependence at temperatures below 15 – 25 K strictly follows Eq. (1) with n = 2. In Fig. 4, the logarithmic resistivity versus $T^{-1/2}$ for sample #2 is plotted.

In Table, the main structure parameters of nanotubes comprising the films, namely, the outer nanotube cage diameter D and the number of carbon layers n_l, as well as the parameters of temperature-dependent resistivity: the measured values of ρ (in units of Ω·cm) at temperatures 5, 25 and 250 K, and the values of n and T_0 in Eq. (1), are summarized for the main types of nanotube films investigated. Also presented is the temperature T^*, above which the experimental $\rho(T)$ dependence notably deviates from Eq. (1).

Attention is drawn to the properties of sample #4. At room temperature, the resistivity of this film containing separate SLT's surrounded by a structureless material is even below that of the films with the bundles of SLT's, but its

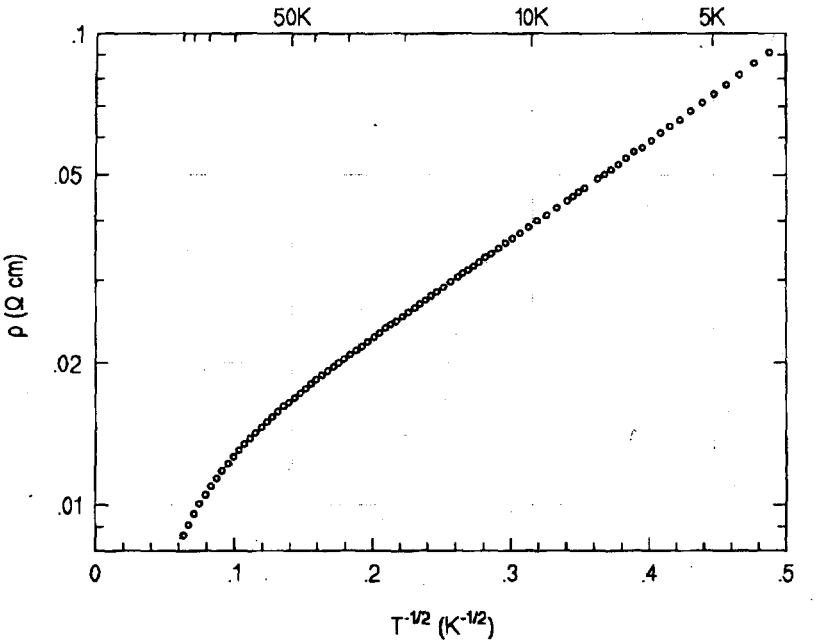

Fig.4. Logarithmic resistivity versus $T^{-1/2}$ for the film with the bundles of SLT's

resistivity $\rho(T)$ at $T < 50\,\mathrm{K}$ follows Eq. (1) with $n = 4$ rather than with $n = 2$ (see Fig. 3, right scale). The value of T_0 therewith is naturally far less than observed in the films containing MLT's.

Thus the $\rho(T)$ dependence with $n = 4$, which is typical of the 3D Mott's conductivity, holds for the films containing either MLT's or separate SLT's surrounded by a structureless material.

From the well known formula for T_0 [15]

$$T_0 = \frac{21.2}{k_B\, N(E_F)\, \xi^3}\ , \tag{2}$$

follows that at density of states at the Fermi level $N(E_F) \sim 10^{18}\ \mathrm{eV}^{-1} \cdot\ \mathrm{cm}^{-3}$ (in accordance with the data for amorphous carbon [16]), the estimated localization length $\xi \sim 6$ nm for the films with MLT's ($T_0 \sim 10^6\,\mathrm{K}$). This is compatible with the mean radius of nanotubes in terms of the order of magnitude. As for another type of films marked by $n = 4$ in Eq. (1), it is apparent that from a very small value of $T_0 \sim 40\,\mathrm{K}$ for sample #4 with separate SLT's follows a vastly greater value of $N(E_F) \sim 6 \cdot 10^{21}\,\mathrm{eV}^{-1} \cdot\ \mathrm{cm}^{-3}$ at $\xi \sim 10$ nm.

It should be noted that the high temperature values of ρ of the films with MLT's are comparable with those of as-prepared activated carbon fibers (ACF) [17]. ACF's are a unique class of porous materials consisting almost exclusively of nanopores of the average size of 1 nm. However, the $\rho(T)$ dependence for as-prepared ACF's follows Eq. (1) with $n = 2$ and $T_0 \sim 500\,\mathrm{K}$ [17]. After heat treatment at $\sim$ 1000 K, a collapse of nanopores occurs that results in a considerable decrease in ρ and T_0. The temperature dependence $\rho(T)$ of these heat-treated ACF's is similar to that of our films containing the bundles of SLT's,

the only difference being that, in our instance, the absolute values of ρ and T_0 are less by an order of magnitude. Besides that, deviations from linearity of the logarithmic resistivity with $T^{-1/2}$ begin at much lower temperature.

The resistivity of granular metals (see, for example, [18]) and of the VRH systems with developing the Coulomb gap in the density of states near the Fermi level [19] is known to follow Eq. (1) with $n = 2$. In the latter case, the equation for T_0 is given by

$$T_0 = \frac{\beta e^2}{k_B \kappa \xi} \ , \tag{3}$$

where e is the electronic charge, κ dielectric constant, and β a dimensionless factors of the order of unity. If we take $T_0 \sim 20\,\mathrm{K}$ (as determined by our measurements) and $\kappa \sim 100$ (that has been estimated for heat-treated ACF [17]), then $\xi \sim 8$ nm, that is again compatible with the radius of the SLT bundle.

Since $N(E_F)$ has not been directly included in Eq. (3), its estimation can be made by use of the experimental T^* value, which can be determined with some degree of certainty marking the temperature where deviation from the linearity of $\ln \rho$ with $T^{-1/2}$ begins. For this purpose, it is necessary to equate the energy interval near the Fermi level

$$\epsilon_0(T) = \frac{(k_B T)^{3/4}}{[N(E_F)\xi^3]^{1/4}} \ , \tag{4}$$

the states of which involve hopping, to the value of the Coulomb gap

$$\Delta = \frac{e^3 N(E_F)^{1/2}}{\kappa^{3/2}} \tag{5}$$

(see, for example, [15]). From the equation $\epsilon_0(T^*) = \Delta$ follows $N(E_F) \sim 5 \cdot 10^{20}\,\mathrm{eV^{-1} \cdot cm^{-3}}$ for $T^* \sim 10\,\mathrm{K}$ and κ and ξ values mentioned above.

In turn, the carrier density $n_c = 2N(E_F)\epsilon_0(T)$, which according to Eq. (4) is proportional to $T^{3/4}$ at low temperatures, can be estimated at $T \sim 25\,\mathrm{K}$ as $n_c \sim 3 \cdot 10^{16}\,\mathrm{cm^{-3}}$ for the films with MLT's, $n_c \sim 1.4 \cdot 10^{19}\,\mathrm{cm^{-3}}$ for the films with separate SLT's, and $n_c \sim 2.5 \cdot 10^{18}\ \mathrm{cm^{-3}}$ for the films with the bundles of SLT's.

In summary it may be said that these simple estimations show that the films containing SLT's (separate or assembled in the bundles) and demonstrating the variable-range hopping conductivity are, in such a situation, the systems with a fairly high ($\sim 10^{21}\ \mathrm{eV^{-1} \cdot cm^{-3}}$) density of states at the Fermi level. Packing of the tubes in ordered assemblies, which are oriented perpendicularly to the substrate, is probably of key importance because it leads to the change of the law governing VRH conductivity at low temperatures from $T^{-1/4}$ to $T^{-1/2}$. This can be interpreted as the appearance of the Coulomb gap in the density of states, that in turn can be a consequence of the assembling of the nanotubes in the bundles. The absence of amorphous substance between the tubules in the bundle, its fairly high homogeneity and an ordered arrangement make it possible to refer to such a bundle as a quasicrystal. It is also possible that these ordered nanotube bundles play a role of metal granules with tunneling between the nearest neighbors. In this case the conductivity also follows the law $-\ln \sigma \propto T^{-1/2}$ [18]. What description would be more appropriate will be seen from further studies of the properties of carbon nanotube films. Among them, the electrical transport in magnetic field should be studied first.

This material is based upon work supported by the Intersectoral Scientific and Technological Program of Russia "Fullerenes and Atomic Clusters" under Grant 4 as well as by the International Scientific and Technological Center under Grant 079. The authors acknowledge useful discussion with A. S. Kotosonov.

---

1. S.Iijima, Nature **354**, 56 (1991).
2. M.S.Dresselhaus, G.Dresselhaus, and P.C.Eklund, J. Mater. Res. **8**, 2054 (1993).
3. S.N.Song, X.K.Wang, R.P.H.Chang, and J.B.Ketterson, Phys. Rev. Lett. **72**, 697 (1993).
4. L.Langer, L.Stockman, J.P. Heremans et al., J. Mater. Res. **9**, 927 (1994).
5. Z.Ja.Kosakovskaja, L.A.Chernozatonskii, and E.A.Fedorov, JETP Lett. **56**, 26 (1992).
6. L.A.Chernozatonskii, E.A.Fedorov, Z.Ja.Kosakovskaja et al., JETP Lett. **57**, 35 (1993).
7. L.A.Chernozatonskii, Z.Ja.Kosakovskaja, A.N.Kiselev, and N.A.Kiselev, Chem. Phys. Lett., **228**, 94 (1994).
8. L.A.Chernozatonskii, Z.Ja.Kosakovskaja, E.A.Fedorov, and V.I.Panov, Phys. Lett. A **197**, 40 (1995).
9. L.A.Chernozatonskii, Yu.V.Gulyaev, Z.Ja.Kosakovskaja et al., Chem. Phys. Lett. **233**, 63 (1995).
10. N.A.Kiselev, L.A.Chernozatoskii, Z.Ja.Kosakovskaja et. al., *Ninth International Conference on Microscopy of Semiconducting Materials, 20–23 March 1995*, University of Oxford, Oxford, 1995.
11. Z.Ja.Kosakovskaja, *Abstracts to 1994 Fall Meeting of Materials Research Society*, page 260.
12. J.M.Cowley, *Diffraction Physics*. North-Holland, Amsterdam, second revised edition, 1990.
13. L.A.Chernozatonskii, Phys. Lett. A **166**, *55* (1992).
14. A.Oberlin, Carbon **17**, 7 (1979).
15. B.I.Shklovskii and A.L.Efros, *Electronic Properties of Doped Semiconductors*, volume 45 of *Springer Series in Solid State Sciences*. Springer, Berlin, 1984.
16. J.J.Hauser, Solid State Comm. **17**, 1557 (1975).
17. A.W.P.Fung, Z.H.Wang, M.S.Dresselhaus et al., Phys. Rev. B, **49**, 17325 (1994).
18. P.Sheng, Philos. Mag., **65**, 357 (1992).
19. A.L.Efros and B.I.Shklovskii, J. Phys. C (Solid State Phys.) **8**, L49 (1975).